Proceedings of the
International Conference on Mechanical Engineering and Renewable Energy 2019
(ICMERE2019) 11 – 13 December, 2019, Chittagong, Bangladesh

ICMERE2019-PI-047

SYNTHESIS, CHARACTERIZATION, AND ENHANCEMENT OF PHOTOCATALYTIC PERFORMANCE OF METHYL BLUE DYE USING Ag/GO DOPED ZnO NANOCOMPOSITE UNDER UV RADIATION

M. R. Al-Mamun[*1], M. S. Islam[1], M. R. Hossain[1], S. Kader[2], M. Z. H. Khan[1]

[1] Dept. of Chemical Engineering, Jashore University of Science and Technology, Jashore 7408, Bangladesh
[2] Dept. of Chemical Engineering, Bangladesh University of Engineering and Technology, Dhaka, Bangladesh
* mamunjust09@gmail.com

Abstract*-In this study, Ag/GO doped ZnO nanocomposites are synthesized by sol-gel and modified thermal heat treatment method. The characterization of Ag/GO/ZnO nanocomposite has been studied by X-ray, SEM, FT-IR, and UV–Vis spectrophotometer for their structure, morphology, functional group, and absorption spectra analysis. The Photocatalytic activity of Ag/GO/ZnO nanocomposites is investigated by the degradation of methylene blue as an organic pollutant based on dye removal under radiation of ultraviolet (UV). The pseudo first-order kinetics is also investigated. The experimental result shows that the ZnO nanoparticles are greatly improved and compared to Ag/GO/ZnO nanocomposite. It expresses that around 99% of MB dye degraded in only 180 minute under UV irradiation. Furthermore, they showed good cyclic performance and easy recovery from the test solution, demonstrating the possibility of their practical use.*

Keywords: Photocatalysis, sol gel, Ag/GO/ZnO nanocomposite, methylene blue, UV irradiation

1. INTRODUCTION

Textile industry is a vital and quickly emerging industrial segment in Bangladesh and play vital role of economic development of the country. At present, around 6000 textile industry grew up in the country, and the export stood around $30 billion per year from this sector [1]. Beside this significant economic benefit from the textile industry, it faces the social and environmental impacts associated with the generations of toxic wastewater from its wet processing operation. Various treatment technologies have been developed for the textile wastewater namely physical, chemical and biological treatment [2-3]. The use of ozone can generate hydroxyl radicals (•OH) that can oxidize a broad range of pollutants non-selectively and the process is known as advanced oxidation processes (AOPs). Advance oxidation processes (AOPs) is considered as one of the most modern technology that is capable of convert unwanted contaminants to harmless products. Literature investigated several AOPs such as Fenton, UV-H_2O_2, UV-ZnO, Solar-ZnO, UV-TiO_2, Solar-TiO_2, O_3-UV, and O3-H_2O_2 [4]. Recently several approaches have been studied to increase the photocatalytic activity of ZnO for textile effluents treatment including metal doping (e.g. Fe, Cu, Al, Cr, Ag, Au, Pt, Pd, Zn, Bi, Mo, Co, Ni, Ce etc.), non-metal doping (e.g. N, C, S, F, I, B etc.) and co-doping with metal/metal (Zn-Cu, Fe-Ni, Y-Dy, Cr-Co, Co-Ni, Ag-Mo, Zn-Eu, etc), metal/non-metal (Pt-N, Mn-P, Y-N, Mo-C, Cu-N, etc) and nonmetal/nonmetal (N-S, B-N, C-F, N-I, etc) with the semiconductor of ZnO [5-9]. The doping of metal/non-metals or co-doping with ZnO nanocomposites has been investigated under UV irradiation with the suspension of batch reactor.

Recently, the deposition of Ag on ZnO nanostructures improve the photocatalytic activity due to stable separation of generated electrons and holes [10]. They demonstrated that only 80 min were needed to fully degrade methylene blue (MB) under UV light using Ag/ZnO nanostructures. The effect of Ag-incorporated ZnO nanostructures have been studied on destroying rhodamine B (RhB) and confirmed an enhancement in photocatalytic efficiency through decoration of ZnO nanostructures [11]. So far, a large amount of work has been carried out to integrate ZnO with carbon-based materials such as CNT, C60, graphite, GO and graphene/rGO. Specifically, two-dimensional (2D) exhibits high electronic conductivity and mobility, high specific surface area and excellent thermal and mechanical properties have been investigated [12].

However, UV-ZnO/Ag/GO nanocomposite is a widely used AOPs for the treatment of textile wastewater because of low cost, stability in aquatic systems, low environmental toxicity and thus it becomes an extremely attractive photocatalyst for the generation of ·OH radical [13-14]. Thus, the proposed technology in combined with the existing conventional technology will assist to remove toxic and bio-persistent dye contaminants effectively and will lead to zero liquid discharge that is not achievable by using the existing technology alone. This paper sequentially represents the synthesis of ZnO/Ag/GO nanocomposite, characterization of nanocomposites, and design of UV photocatalytic reactor.

Then finally, the photocatalytic activity of UV-ZnO/Ag/GO nanocomposite process for the treatment of azo dye (Methylene Blue) with optimization based on dye removal has been studied.

2. MATERIALS AND METHODOLOGY

2.1 Materials

Zinc acetate dehydrate ($Zn(CH_3COO)_2{\cdot}2H_2O$), sodium hydroxide (NaOH), graphene oxide (GO) solution ethanol (C_2H_5OH) and hydrochloric acid (HCl) were purchased from Merck life science private limited. Silver nitrate ($AgNO_3$) was purchased from Merck KGaA64271 Darmsladt. Methylene blue ($C_{16}H_{18}ClN_3S$) was purchased from BDH Chemicals Ltd, Poole England.

2.2 Preparation of Zinc Oxide Nanoparticle

ZnO nanoparticle are synthesized by sol gel method using zinc acetate dehydrate and sodium hydroxyl. Zinc nitrate (0.2 M), 8.78gm is dissolved in 200 ml of distilled water and is kept under constant stirring for 15 min to complete dissolution, then the solution (0.1M), 0.8gm of NaOH is mixed with distilled water respectively [15]. The NaOH solution is slowly added into zinc acetate dehydrate solution at room temperature under vigorous stirring, which results in the formation of a white precipitation. The white precipitation product is centrifuged at 4000 rpm and washed with distilled water several times to form a nanoparticle. Then the collected precipitated are dried at 90°C (1hr), 100°C (1hr), 110°C (1hr). And finally the obtained product is calcined at 400 °C in Muffle furnace for 2 hours.

2.3 Preparation of Silver Doped Zinc Oxide Nanoparticle

ZnO/Ag nanocomposite are synthesized by sol gel method using zinc acetate dehydrate and sodium hydrosyl. Zinc nitrate (0.2M), 8.78gm is dissolved in 200 ml of distilled water and is kept under constant stirring for 15 min to complete dissolution, then the solution (0.1M), 0.8gm of NaOH is mixed with distilled water respectively. The NaOH solution is slowly added into zinc acetate dehydrate solution at room temperature under vigorous stirring. Then (0.1 M) $AgNO_3$, 1.34gm is dissolved in 80 ml of water and added to the previous solution with continuous stirring carefully that the resulting formation leads to precipitate [16]. The white precipitate product is centrifuged at 4000 rpm and washed with distilled water several times to form a nanocomposie. Then the collected precipitated are dried at 90°C (1hr), 100°C (1hr), 110°C (1hr). And finally the obtained product is calcined at 400°C in Muffle furnace for 2 hours.

2.4 Preparation of Silver and GO co-doped Zinc Oxide Nanoparticle

ZnO/Ag/GO nanocomposite are synthesized by sol gel method using zinc acetate dehydrate and sodium hydroxyl. Zinc nitrate (0.2M), 8.78gm is dissolved in 200 ml of distilled water and is kept under constant stirring for 15 min to complete dissolution, then the solution (0.1M), 0.8gm of NaOH is mixed with distilled water respectively. Then the prepared 0.01wt% GO (0.46ml) solution is dissolved in 60ml of ethanol and is kept under constant stirring for 15 min to complete dissolution [17]. Then the solution is sonication for 40 min in sonicator carefully. Then the GO solution is added to the previous solution at room temperature under vigorous stirring. Then prepared 0.1M $AgNO_3$, 80 ml of water added to the solution with continuous stirring and keep it rest under room temperature for 1days. Then the resulting formation leads to a blackish precipitation. The blackish precipitation product is centrifuged at 4000 rpm and washed with distilled water several times. The collected precipitated are dried at 90°C (1hr), 100°C (1hr), 110°C (1hr). And finally, the obtained product is calcined at 400°C in Muffle furnace for 2 hours.

3. PHOTOCATALYTIC EXPERIMENT

The UV/ZnO suspension experiments are carried out in a batch reactor with the influence of solution pH, photocatalyst dosage and initial dye concentration. The 125 ml of methylene blue dye solution is placed into the cylindrical Pyrex cell of 250 cm^3 beakers with the different doses of ZnO/Ag/GO nanocomposites. The experiments are conducted at surrounding room temperature. There are 5 UV lights containing each of 20W are used as light source. The oxidation is performed with fixed initial dye concentration of 15 ppm at 125 ml solution and fixed pH of 8 with the help of UV irradiation. The pH is regulated by adding incremental amounts of either dilute HNO_3 or NaOH to the solution. The photocatalyst material is kept in the beaker with the continuous magnetic stirring. The magnetic stirring speed is maintained at medium speed throughout the study to ensure equilibrium is reached. At the end of preset time intervals, samples are withdrawn and the changes in concentration of dye solution is analyzed by using UV-vis spectrophotometer. The batch reactor studies are also carried out at surrounding temperature of interval 11.00 am to 2.00 pm.

The percentage (%) degradation is calculated as follows:

$$\% \text{ Degradation} = \frac{C_O - Ct}{C_O} \times 100 \quad \text{..... (3.1)}$$

Where C_0 = initial concentration of dye solution, Ct = concentration of dye solution after irradiation.

Rate constant equation:

$$\ln\left(\frac{C_t}{C_o}\right) = -kt$$

$$k = \ln\left(\frac{C_t}{C_o}\right)/(-t) \quad \text{..... (3.2)}$$

Where C_0 is the initial concentration of dye, and C_t is the concentration of dye at reaction time t (min).

4. RESULTS AND DISCUSSIONS

4.1 Characterization

The analytical techniques used in this research work for characterization of ZnO/Ag/GO photocatalyst are UV-Vis Spectroscopy, Fourier Transform Infrared Spectroscopy (FT-IR), X-ray Diffraction (XRD), Scanning Electron Microscopy (SEM) analysis. The analytical results obtained are discussed in this particular section with respect to performed test in the laboratories.

4.1.1 Ultraviolet-Visible Spectroscopy (UV-Vis) of ZnO/Ag/GO Nanocomposite

The photocatalyst of ZnO/Ag/GO nanocomposites are monitored by UV–Vis spectrophotometer in the range of 200–800 nm for obtaining the maximum absorbance with respect wavelength [18]. The 1 mg samples of ZnO, ZnO-Ag, ZnO-Ag-GO nanocomposites are dissolved in 10 ml distilled water with continuous stirring carefully. The maximum absorbance of with respect wavelength of ZnO, ZnO/Ag, ZnO/Ag/GO nanocomposites are shown in the Figure 4.1.

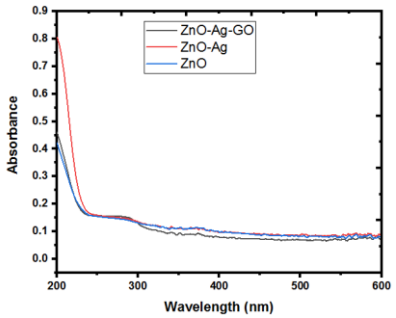

Fig. 4.1: Ultraviolet-Visible Spectroscopy of ZnO, ZnO/Ag, ZnO/Ag/GO nanocomposites

4.1.2 Fourier Transform Infrared Spectroscopy Study

Doping of metals into zinc oxide changes the intensity of peaks as it can be seen in all samples. Therefore, in all cases the peaks of 3020 cm^{-1} to 3440 cm^{-1} corresponding to the OH transfers and reacts with free radicals available in the dye which leads to the photocatalytic oxidation of the dye. The bands at 2900 cm^{-1} and 2940 cm^{-1} are attributed to C-H bending and stretching mode [19]. The broad absorption in the range of 1585 cm^{-1} is assigned to the bending vibration and stretching mode of water and hydroxyl groups on the surface of the samples. The peaks from 464 cm^{-1} to 474 cm^{-1} represent the stretching vibration of ZnO in all cases. On doping with silver, stronger and wider absorption bands are observed in the region of ~ 676 cm^{-1}. The absorbance bands of ZnO, ZnO/Ag, ZnO/Ag/GO nanocomposites are shown in the Figure 4.2.

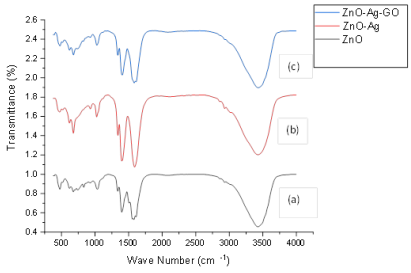

Fig. 4.2: FTIR spectra of (a) ZnO (b) Ag doped ZnO (c) Ag and GO co-doped ZnO photocatalysts

4.1.3 Scanning Electron Microscopy (SEM)

To investigate the morphology and particle size of ZnO, ZnO/Ag, ZnO/Ag/GO nanocomposite, SEM images are taken and presented in the Figure 4.3. The most morphology of the single particle is columnar in shape. There is a significant change in the surface morphology of ZnO, ZnO/Ag, ZnO/Ag/GO thin film are shown. It can be seen that Ag-doped ZnO has a porous surface which is important for the photocatalytic application [20]. The Ag content strongly affects the ZnO surface. The average particle size distributions of ZnO, ZnO/Ag, ZnO/Ag/GO nanocomposites are 80-90, 60-70, and 75-85 nm respectively.

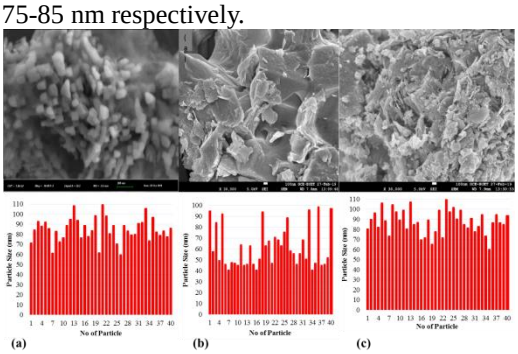

Fig. 4.3: SEM and particle size distribution of (a) ZnO, (b) Ag/ZnO, and (c) Ag/GO/ZnO

4.1.4 X-Ray Diffraction

The XRD analysis is employed to identify the phase structure and the purity of the photocatalysts. The XRD patterns of commercial ZnO and prepared Ag/ZnO photocatalysts are recorded [21]. The results showed in Figure 4.4 (a), (b), and (c) evidenced strong diffraction peaks indicating that the synthesized products have high crystallinity. All the prepared samples have the typical hexagonal Wurtzite structure of ZnO with 2-Theta; diffraction peaks at 31.7°, 34.5°, 36.2°, 47.7°, 56.84°, 63°, 68.1° in Figure 4.4(a) corresponding to (100), (002), (101), (102), (110), (103) and (112) planes, respectively. The maximum diffraction intensity was observed at 36.2°. Ag/ZnO samples revealed three smalls additional diffraction peaks at 38.2°, 44.2°, and 64.5° that correspond to (111), (200), and (220) crystal planes due to the presence of Ag in Figure 4.4(b). These peaks are associated with the face-centered-cubic phase of metallic Ag. No characteristic peaks of impurity phases, such as silver oxide phases, were observed from the patterns. The main peaks of the XRD pattern of Ag/GO/ZnO nanocomposite are shown in Figure 4.4(c).

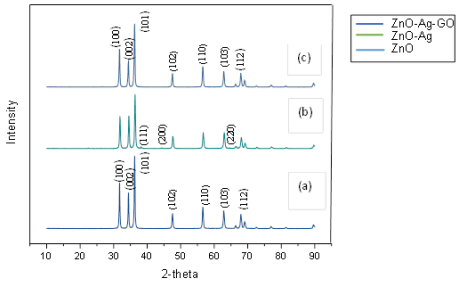

Fig. 4.4: XRD spectra of (a) ZnO (b) Ag doped ZnO (c) Ag doped GO co-doped ZnO photocatalysts

4.2 Effect of Concentration on photocatalytic Degradation of Methylene Blue Based on Doses

The effects of concentration on photocatalytic degradation of MB dye based on doses are studied. The amount of photocatalyst is varied from 0.05 to 0.35gm per 125 ml of constant dye solution of 15 ppm concentration and pH was 8.0. We observe that with increasing catalyst amounts degradation of MB increases due to increase in the number of active surfaces on the catalyst and attains maximum value at an optimum

photocatalyst load (here 0.300 gm per 125 ml solution). Maximum concentration of MB dye from 15.00 to 0.0867 ppm is achieved at 3 h under UV irradiation using 0.350 gm ZnO photocatalysts. Similarly, Maximum concentration of MB dye from 15.00 to 0.1099 ppm is achieved at 3 h under UV irradiation using 0.350 gm ZnO/Ag photocatalysts. And finally, Maximum concentration of MB dye from 15.00 to 0.0145 ppm is achieved at 3 h under UV irradiation using 0.350 gm ZnO/Ag/GO photocatalysts. The effects of concentration based on doses are shown in the Figure 4.5 (a), (b), and (c).

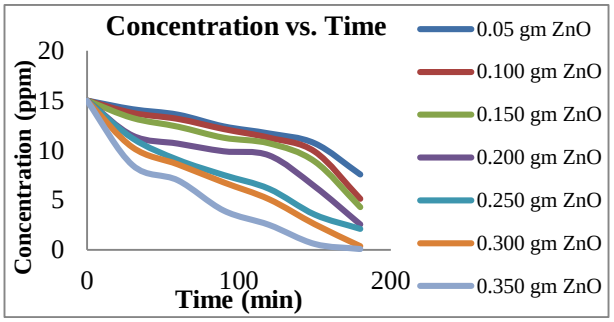

Fig. 4.5: (a) Effect of dye concentration for degradation of MB by using ZnO photocatalyst

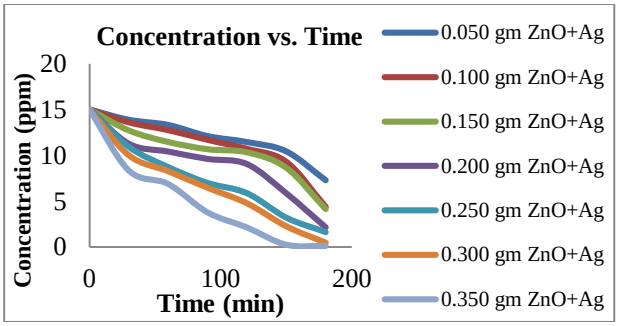

Fig. 4.5: (b) Effect of dye concentration for degradation of MB by using ZnO/Ag photocatalyst

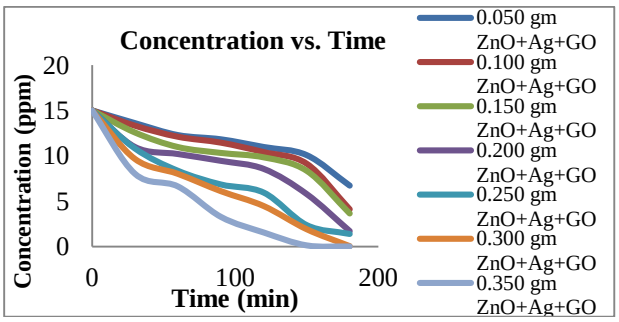

Fig. 4.5: (c) Effect of dye concentration for degradation of MB by using ZnO/Ag/GO photocatalyst

4.3 Effect of Dye Removal for the Photocatalytic Degradation of Methylene Blue

The effects of dye removal on photocatalytic degradation of MB dye based on doses are studied. The amount of photocatalyst was varied from 0.05 to 0.35gm per 125 ml of constant dye solution of 15 ppm concentration and pH is 8.0. The removal percentage of MB dye are 49.53, 65.73, 71.35, 82.95, 86.09, 97.61, and 99.42 for 0.050 gm, 0.100 gm, 0.150 gm, 0.200 gm, 0.250 gm, 0.300 gm, 0.350 gm ZnO photocatalyst respectively under 180 min contact time. Similarly, The removal percentage of MB dye are 51.39, 70.88, 72.48, 85.78, 89.23, 98.79, and 99.86 for 0.050 gm, 0.100 gm, 0.150 gm, 0.200 gm, 0.250 gm, 0.300 gm, 0.350 gm ZnO/Ag photocatalyst respectively under 180 min contact time. Finally, The removal percentage of MB dye are 55.26, 72.53, 75.67, 88.51, 90.78, 99.53, and 99.90 for 0.050 gm, 0.100 gm, 0.150 gm, 0.200 gm, 0.250 gm, 0.300 gm, 0.350 gm ZnO/Ag/GO photocatalyst respectively under 180 min contact time. The effects of removal percentage based on doses are shown in the Figure 4.6 (a), (b), and (c).

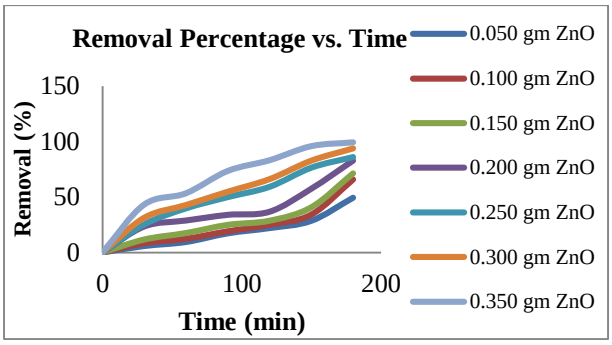

Fig. 4.6: (a) Effect of removal percentage based on photocatalyst doses of ZnO in MB dye

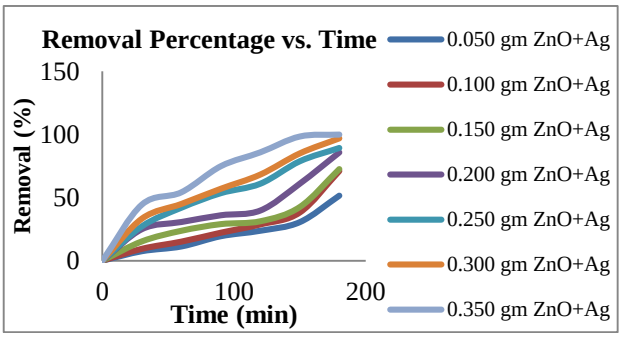

Fig. 4.6: (b) Effect of removal percentage based on photocatalyst doses of ZnO/Ag in MB dye.

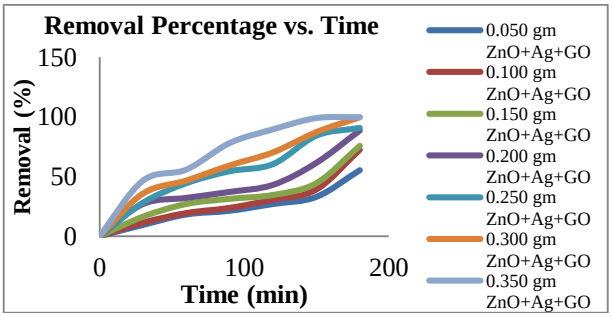

Figure 4.6: (c) Effect of removal percentage based on photocatalyst doses of ZnO/Ag/GO in MB dye

4.4 Effect of Pseudo First-order Kinetics on the Photocatalytic Degradation of Methylene Blue

The corresponding graphs for different photocatalysts

reaction kinetics are plotted as shown in Figure 4.7 (a), (b), (c). The respective photocatalytic reaction rate constants are calculated from the slope of linear trend-line plot. The respective rate constants for photocatalytic MB dye degradation of 0.050 gm, 0.100 gm, 0.150 gm, 0.200 gm, 0.250 gm, 0.300 gm, and 0.350 gm photocatalyst doses of ZnO are found to be 0.0033 min^{-1}, 0.0048 min^{-1}, 0.0056 min^{-1}, 0.0079 min^{-1}, 0.0103 min-1, 0.0173 min^{-1}, and 0.0259 min^{-1} respectively. Similarly, the respective rate constants for photocatalytic MB dye degradation of ZnO/Ag are found to be 0.0034 min^{-1}, 0.0055 min^{-1}, 0.0057 min^{-1}, 0.0087 min^{-1}, 0.0114 min^{-1}, 0.014 min^{-1} and 0.0334 min^{-1} respectively. Finally, the respective rate constants for photocatalytic MB dye degradation of ZnO/Ag/GO are found to be 0.0037 min^{-1}, 0.0057 min^{-1}, 0.0062 min^{-1}, 0.0095 min^{-1}, 0.0125 min^{-1}, 0.0237 min^{-1}, and 0.0362 min^{-1} respectively. It demonstrates that the straight lines almost fit the experimental values. The slight deviations might be due to operating conditions like light intensity, oxygen concentration or interfering intermediates.

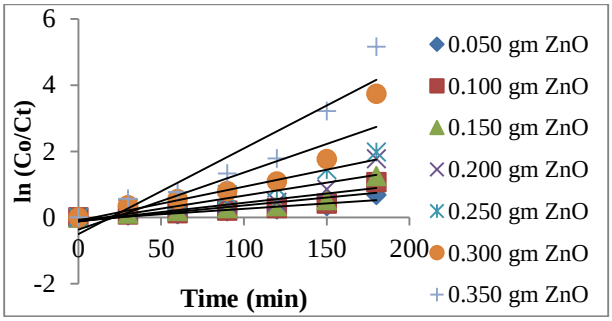

Fig. 4.7: (a) Pseudo first-order kinetics of MB dye under UV irradiation by using ZnO nanoparticle

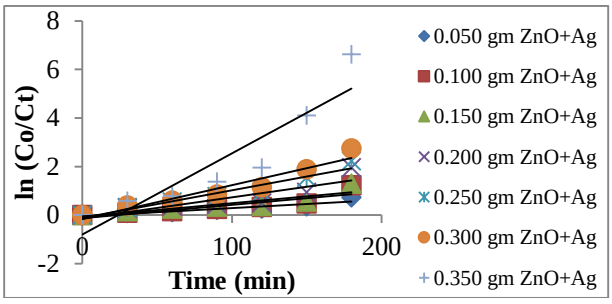

Fig. 4.7: (b) Pseudo first-order kinetics of MB dye under UV irradiation by using ZnO/Ag nanoparticle

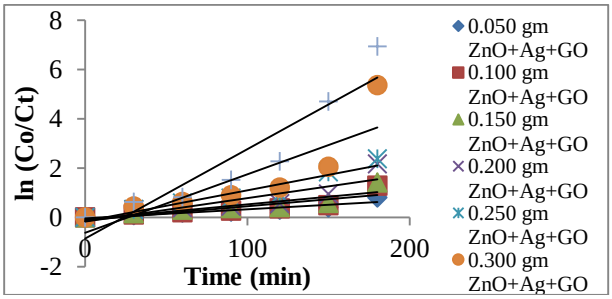

Fig. 4.7: (c) Pseudo first-order kinetics of MB dye under UV irradiation by using ZnO/Ag/GO nanoparticle

5. CONCLUSION

In this study, we have used modified sol gel method with thermal treatment method for the fabrication of ZnO nanocomposite along with Ag and GO doping. The photocatalytic performance of MB dye in presence of UV radiation has been investigated with contact time of 180 min. The optimum dopant of Ag and Go is 0.10 wt%, and 0.01 wt% respectively. The optimum dye concentration and pH was 15 ppm and 8.0 respectively. The photocatalytic degradation MB dye is about 93.94%, 96.79% and 99.53 % have been found with optimum photocatalyst doses of 0.300 gm, ZnO, Ag/ZnO, and Ag/GO/ZnO respectively under UV irradiation. The experimental suggests that the Ag and Go co-doped ZnO nanocomposite shows the higher potential for the treatment of textile wastewater in addition with exiting treatment.

6. REFERENCES

[1] C. R. Holkar, A. J. Jadhav, D. V. Pinjari, N. M. Mahamuni, and A. B. Pandit, "A critical review on textile wastewater treatments: Possible approaches", *Journal of Environment Management*, vol. 182, pp. 351–366, 2016.

[2] R. Ganesh, G. D. Boardman, and D. Michelson, "Fate of azo dyes in sludges", *Waste Water Research*, vol. 28, pp. 1367–1376, 1994.

[3] E. J. Weber, and R. L. Adams, "Chemical and sediment mediated reduction of the azo dye disperse blue 79", *Environmental Science Technology*, vol. 29, pp. 1163–1170, 1995.

[4] C. G. da Silva, and J. L. Faria, "Photochemical and photocatalytic degradation of an azo dye in aqueous solution by UV irradiation", *Journal of Photochemical and Photobiology A: Chemistry*, vol. 155, no. 1-3, pp. 133–143, 2003.

[5] P. Pascariu, I. V. Tudose, M. Suchea, E. Koudoumas, N. Fifere, and A. Airinei, "Preparation and characterization of Ni, Co doped ZnO nanoparticles for photocatalytic applications", *Applied Surface Science*, vol. 448, pp. 481-488, 2018.

[6] R. Mahdavi, and S. S. A. Talesh, "Sol-gel synthesis, structural and enhanced photocatalytic performance of Al doped ZnO nanoparticles", *Advanced Powder Technology*, vol. 28, no. 5, pp. 1418–1425, 2017.

[7] P. K. Labhane, S. H. Sonawane, G. H. Sonawane, S. P. Patil, and V. R. Hus, "Influence of Mg doping on ZnO nanoparticles decorated on graphene oxide (GO) crumpled paper like sheet and its high photo catalytic performance under sunlight", *Journal of Physics and Chemistry of Solids*, vol. 114, pp. 71–82, 2018.

[8] S. Benzitouni, M. Zaabat, M. S. Aida, J. Ebothe, J. Michel, B. Boudine, L. Mansouri, and T. Saidani, "Morphology and photocatalytic activity of porous (In, Mg) codoped ZnO nanoparticles", *Optik-International Journal for Light and Electron Optics* (2010), https://doi.org/10.1016/j.ijleo.2017.12.039

[9] S. M. Hosseini, I. A. Sarsari, P. Kameli, and H. Salamati, "Effect of Ag doping on structural, optical, and photocatalytic properties of ZnO nanoparticles",

Journal of Alloys and Compounds, vol. 640, pp. 408–415, 2015.

[10] W. Xie, Y. Li, W. Sun, J. Huang, H. Xie, and X. Zhao, "Surface modification of ZnO with Ag improves its photocatalytic efficiency and photostability", *Journal of Photochemical and. Photobiology A*, vol. 216, pp. 149-155, 2010.

[11] H. Liu, G. Shao, J. Zhao, Z. Zhang, Y. Zhang, J. Liang, X. Liu, H. Jia, and B. Xu, "Worm-like Ag/ZnO core-shell heterostructural composites: fabrication, characterization, and photocatalysis", *Journal of Physical Chemistry C*, vol. 116, pp. 16182-16190, 2012.

[12] Y. Zhao, L. Liu, T. Cui, G. Tong, and W. Wu, "Enhanced photocatalytic properties of ZnO/reduced graphene oxide sheets (rGO) composites with controllable morphology and composition", *Applied Surface Science*, vol. 412, pp. 58–68, 2017.

[13] D. B. Bharti, and A. V. Bharati, "Photocatalytic degradation of Alizarin Red dye under visible light using ZnO & CdO nanomaterial", *Optik*, vol. 160, pp. 371–379, 2018.

[14] R. Mahdavi, and S. S. A. Talesh, "Sol-gel synthesis, structural and enhanced photocatalytic performance of Al doped ZnO nanoparticles", *Advanced Powder Technology*, vol. 28, pp. 1418–1425, 2017.

[15] L. V. Trandafilovi, D. J. Jovanovi, X. Zhang, S. Ptasi´nsk, and M. D. Drami´canin, "Enhanced photocatalytic degradation of methylene blue and methylorange by ZnO:Eu nanoparticles", *Applied Catalysis B: Environmental*, vol. 203, pp. 740–752, 2017.

[16] Q. T. H. Ta, S. Park, and J. S. Noh, "Ag Nanowire/ZnO Nanobush Hybrid Structures for Improved Photocatalytic Activity", *Journal of Colloid and Interface Science*, (2017), doi: http://dx.doi.org/10.1016/j.jcis.2017.06.041

[17] A. Pruna, Z. Wu, J. A. Zapien, Y. Y. Li, and A. Ruotolo, "Enhanced photocatalytic performance of ZnO nanostructures by electrochemical hybridization with graphene oxide", *Applied Surface Science* (2018), doi: https://doi.org/10.1016/j.apsusc.2018.02.117

[18] R. Muñoz-Espí, G. Jeschke, I. Lieberwirth, C. M. Gómez, and G. Wegner, "ZnO− Latex Hybrids Obtained by Polymer-Controlled Crystallization: A Spectroscopic Investigation", *The Journal of Physical Chemistry B*, vol. 111, pp. 697-707, 2007.

[19] D. Scarano, S. Bertarione, G. Spoto, A. Zecchina, and C. O. Arean, "FTIR spectroscopy of hydrogen, carbon monoxide, and methane adsorbed and co-adsorbed on zinc oxide", *Thin Solid Films*, vol. 400, pp. 50-55, 2001.

[20]F. Ahmed, N. Arshi, M. Anwar, R. Danish, and B. H. Koo, "Morphological evolution of ZnO nanostructures and their aspect ratio-induced enhancement in photocatalytic properties", *RSC Advances*, vol. 4, pp. 29249-29263, 2014.

[21] T. Kawano, and H. Imai, "A simple preparation technique for shape-controlled zinc oxide nanoparticles: Formation of narrow size-distributed nanorods using seeds in aqueous solutions", *Colloids and Surfaces A: Physicochemical and Engineering Aspects*, vol. 319, pp. 130-135, 2008.